



Electronic orbital currents and polarization in Mott insulators

L. N. Bulaevskii and C. D. Batista

Los Alamos National Laboratory, Los Alamos, New Mexico 87545, USA

M. V. Mostovoy

Groningen University, Nijenborgh 4, 9747AG Groningen, The Netherlands

D. I. Khomskii*

Physikalisches Institut, Universität zu Köln, Zùlpicher Strasse 77, D-50937 Köln, Germany

(Received 14 August 2007; published 1 July 2008)

Strongly correlated electron insulators are one of the most important classes of materials in modern solid-state physics. We demonstrate that certain classes of Mott insulators, that usually are geometrically frustrated, exhibit unexpected charge effects: for certain spin textures, *spontaneous circular electric currents* or *nonuniform charge distribution* exist in the ground state of Mott insulators. In addition, low-energy “magnetic” states contribute comparably to the dielectric and magnetic response functions, $\epsilon_{ik}(\omega)$ and $\mu_{ik}(\omega)$, leading to interesting phenomena such as dipole-active ESR transitions, rotation of the electric-field polarization, and resonances which may be common to both functions producing a negative refraction index in a window of frequencies.

DOI: [10.1103/PhysRevB.78.024402](https://doi.org/10.1103/PhysRevB.78.024402)

PACS number(s): 72.80.Sk, 74.25.Ha, 73.22.Gk

I. INTRODUCTION

Mott insulators are the paradigm of strongly correlated materials. Very important materials belong to this class such as the parent compounds for the High-Tc cuprates, colossal-magnetoresistance manganites, and most of the quantum magnets. Their minimal Hamiltonian is the Hubbard model which includes a hopping term, t , and on-site Coulomb interaction U . At half filling (one electron per site) and in the large U/t limit, each site is occupied by a single electron to avoid the strong on-site repulsion. The charge becomes localized by this mechanism and the low-energy properties are described by the remaining spin degrees of freedom. For this reason, Mott insulators with large U/t have been traditionally considered as materials which have only magnetic properties at low energies due to their spin moments. Despite this common conviction, we will show here that certain Mott insulators exhibit real electric currents in loops (orbital currents) that produce orbital magnetic moments. Other spin textures lead to a modulation of the electron charge, i.e., the electronic density at a given site i can be different from one: $\langle n_i \rangle \neq 1$. In particular, this can lead to an electric polarization, i.e., to a purely electronic mechanism of multiferroic behavior.¹⁻⁵

In most cases, the orbital currents are a physical manifestation of the scalar chirality that appears in numerous discussions of superconducting and magnetic systems⁶⁻¹⁵ and is defined as the average value of:

$$\chi_{12,3} = \mathbf{S}_1 \times \mathbf{S}_2 \cdot \mathbf{S}_3, \quad (1)$$

where \mathbf{S}_i is the spin operator on site i . Particularly interesting is the case of spin orderings with zero average moment, $\langle \mathbf{S}_i \rangle = 0$, and nonzero scalar spin chirality $\langle \chi_{12,3} \rangle \neq 0$. Such situation can occur naturally in two-dimensional $SU(2)$ invariant systems because the order parameter $\langle \mathbf{S}_i \rangle \neq 0$ cannot survive thermal fluctuations according to the Mermin-

Wagner theorem.¹⁶ In contrast, the order parameter $\langle \chi_{12,3} \rangle$ can be nonzero at finite temperature because it only breaks discrete symmetries.^{11,12,17,18}

Besides unveiling the physical meaning of the scalar chirality, the existence of net orbital currents (and electric-dipole moments) has several consequences for Mott insulators. Spins are coupled not only to a magnetic field but also to an electric field. Moreover, nonvanishing matrix elements of the polarization between the ground state and excited magnetic states result in a nonvanishing contribution to the dielectric tensor, $\epsilon_{ik}(\omega)$, at low energies, with optical strengths comparable to those of the magnetic-susceptibility tensor $\mu_{ik}(\omega)$.

The apparent contradiction between the insulating nature of the system and the existence of nonzero orbital currents is resolved when we notice that electrons are not completely localized on their ions for finite U/t . In fact, the effective Heisenberg interaction, $J \propto t^2/U$, results from a partial delocalization: an electron gains kinetic energy by “visiting” virtually a neighboring site, but this only occurs if the spins are opposite on both sites (Pauli’s principle). Similarly, the electron can move along a closed loop generating local currents that depend on the spin structure along the loop.

II. CHARGE EFFECTS IN MAGNETIC STATES

We start by considering a half-filled Hubbard model on a general lattice:

$$H = - \sum_{ij\sigma} t_{ij} (c_{i\sigma}^\dagger c_{j\sigma} + c_{j\sigma}^\dagger c_{i\sigma}) + \frac{U}{2} \sum_i (n_i - 1)^2, \quad (2)$$

where sites are labeled by indices i, j , $c_{i\sigma}^\dagger$ ($c_{i\sigma}$) is the creation (annihilation) operator of an electron with spin σ on site i and $n_i = \sum_\sigma c_{i\sigma}^\dagger c_{i\sigma}$ is the number operator. For $t_{ij} = 0$, the lowest-energy eigenstates, $|\tilde{\psi}_i\rangle$, of the Hamiltonian are the

2^N (spin degeneracy) states with one electron per site (N is the number of sites). The excited or polar eigenstates have at least one double-occupied site and they are separated from the 2^N -degenerate ground state by a gap nU , where n is the number of double-occupied sites. As t_{ij} becomes nonzero, the spin degeneracy is lifted because the lowest-energy subspace is mixed with the polar states. The new 2^N states, $|\psi_\nu\rangle = e^{-S}|\tilde{\psi}_\nu\rangle$, that are adiabatically connected with the states, $|\tilde{\psi}_\nu\rangle$, via the unitary transformation e^{-S} , generate the subspace \mathcal{S} of “magnetic” states. The projection of H into \mathcal{S} leads to an effective low-energy Heisenberg spin Hamiltonian, $\tilde{H} = Pe^SHe^{-S}P$, (P is the projector on the \mathcal{S} subspace), which is obtained by standard degenerate perturbation theory in $t/U \ll 1$ and acts on the states $|\tilde{\psi}_\nu\rangle$. Consequently, \tilde{H} is expressed in terms of spin operators:

$$S_i^\eta = \sum_{\mu,\nu} c_{i\mu}^\dagger \sigma_{\mu\nu}^\eta c_{i\nu}, \quad (3)$$

where σ^η are the Pauli matrices and $\eta = \{x, y, z\}$. The expression of \tilde{H} to order t^2 is:

$$\tilde{H}^{(2)} = \sum_{ij} J_{ij} (\mathbf{S}_i \cdot \mathbf{S}_j - 1/4), \quad (4)$$

with $J_{ij} = 4t_{ij}^2/U$ (the usual superexchange). To describe the physical properties of magnetic states, it is convenient to project not only the Hamiltonian but also any other physical operator, O , in order to obtain the effective operator, $\tilde{O} = Pe^SOe^{-S}P$, that acts on the states $|\tilde{\psi}_\nu\rangle$: $\langle\psi_i|O|\psi_j\rangle = \langle\tilde{\psi}_i|\tilde{O}|\tilde{\psi}_j\rangle$ (see Appendix). The effective operator \tilde{O} is always a function of the spin operators \mathbf{S}_i .

We will consider first the current operator

$$\mathbf{I}_{ij} = \frac{iet_{ij}\mathbf{r}_{ij}}{\hbar r_{ij}} \sum_{\sigma} (c_{j\sigma}^\dagger c_{i\sigma}^\bullet - c_{i\sigma}^\dagger c_{j\sigma}) \quad (5)$$

between sites i and j . Since the shortest loop is a triangle, the lowest-order nonvanishing contribution to the current operator is t^3/U^2 and contains the product of three spin operators. The current is a scalar under spin rotations and it is odd under time reversal and under spatial inversion. The only possible expression involving three spin operators is the scalar chirality operator (1). Using perturbation theory,¹⁹ (see Appendix), we find that the contribution to the current in the bond 1,2 from the triangle 1–2–3 is:

$$\tilde{\mathbf{I}}_{1,2,3} = \frac{\mathbf{r}_{12}}{r_{12}} \frac{24e}{\hbar} \frac{t_{12}t_{23}t_{31}}{U^2} [\mathbf{S}_1 \times \mathbf{S}_2] \cdot \mathbf{S}_3. \quad (6)$$

Equation (6) shows that a net scalar spin chirality leads to a net orbital current circulating in the corresponding triangle [see Fig. 1(a)].²⁰ This current produces an orbital magnetic moment $\tilde{\mathbf{L}}_{ijk} \propto \chi_{ij,k} \hat{\mathbf{z}}$, where $\hat{\mathbf{z}}$ is normal to the plane of the triangle. Equation (6) explains the origin of the linear coupling between magnetic field and $\chi_{ij,k}$ found by Motrunich²¹ in the spin Hamiltonian \tilde{H} when a nonzero vector potential is included in H . We note that orbital currents only appear for noncoplanar magnetically ordered states, as \tilde{L}_z is propor-

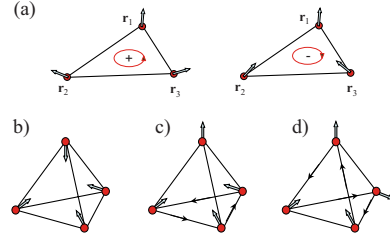


FIG. 1. (Color online) (a) Ground states with nonzero electric current of the C_3 invariant Heisenberg triangle. The circular arrows indicate circular currents, and (+, -) indicate the sign of the scalar chirality. (b)–(d) Noncoplanar spin configuration in a pyrochlore lattice. (b) Four spins point inward along the principal diagonals; the net currents are zero. (c) Three spins point inward while the other one points outwards leading to a net current circulating in the opposite triangle. (d) Two spins point inward and the other two point outward. The orbital current circulates in a loop formed by four edges of the tetrahedron.

tional to a solid angle formed by the spin vectors $\langle\mathbf{S}_1\rangle$, $\langle\mathbf{S}_2\rangle$, and $\langle\mathbf{S}_3\rangle$.

The orientation of the orbital moments depends on the spin texture and on the signs of t_{ij} . It is important to note that for extended lattices the current on a given bond is the sum of the loop currents in all the triangles to which that bond belongs: $\tilde{\mathbf{I}}_{ij} = (\mathbf{r}_{ij}/r_{ij}) \sum_k I_{ij,k}$. In some particular cases, the net current on the bond is zero because different contributions cancel each other. For instance, two-dimensional systems may have no currents inside the crystal although a net current appears on the perimeter (see Fig. 2).

In contrast, currents do not exist necessarily on the surface of three-dimensional systems. The regular $S=1/2$ single-tetrahedron with antiferromagnetic Heisenberg interactions²² provides the simplest example of this situation. The two singlet ground states can be chosen to have nonzero (and opposite) scalar chirality,⁶ while the net current on each bond is zero. The same is true for the “four in” or “four out” structure [Fig. 1(b)] that results for higher spins in presence of a strong uniaxial $[\pm 1, \pm 1, \pm 1]$ anisotropy. However, the structures “three in–one out” or “two in–two out” (spin ice), which can be stabilized by an external field, have nonzero net orbital currents as shown in Figs. 1(c) and 1(d).

In a similar way, we derive an expression for the projected local electron number operator \tilde{n}_i . This operator is a scalar under rotations in spin space, i.e., it must be a function of the combinations $\mathbf{S}_i \cdot \mathbf{S}_j$. The first nonzero contribution to a deviation $\delta\tilde{n}_i$ from unity is (see Appendix)

$$\delta\tilde{n}_1 = \tilde{n}_1 - 1 = 8 \frac{t_{12}t_{23}t_{31}}{U^3} [\mathbf{S}_1 \cdot (\mathbf{S}_2 + \mathbf{S}_3) - 2\mathbf{S}_2 \cdot \mathbf{S}_3]. \quad (7)$$

A similar expression holds for the charges at sites 2 and 3 after a cyclic permutation of indices. The spin structure of the charge operator is uniquely fixed by the invariance of \tilde{n}_1 under time-reversal symmetry and the interchange of sites 2 and 3, as well as by the conservation of total charge of the triangle: $\sum_{i=1}^3 \delta\tilde{n}_i = 0$. Hence, the average electron density at a given site of a Mott insulator depends on the spin structure and is not necessarily equal to one.

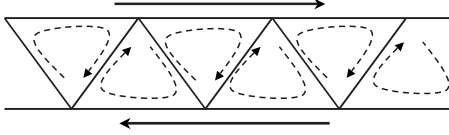


FIG. 2. Example of a system with uniform scalar spin chirality but no net currents in the interior bonds due to cancellation between the contributions from adjacent triangles (dashed arrows). A net current (full arrows) appears on the perimeter because such bonds belong to only one triangle.

The charge redistribution in a single equilateral triangle induces an electric dipole in magnetic states [see Fig. 3(a)]:

$$\begin{aligned}\tilde{P}_x &= 4\sqrt{3}ea(t/U)^3[\mathbf{S}_1 \cdot (\mathbf{S}_2 + \mathbf{S}_3) - 2\mathbf{S}_2 \cdot \mathbf{S}_3], \\ \tilde{P}_y &= 12ea(t/U)^3\mathbf{S}_1 \cdot (\mathbf{S}_2 - \mathbf{S}_3),\end{aligned}\quad (8)$$

where a is the distance between sites.

For an extended lattice, these electric dipoles can appear spontaneously or can be induced by a magnetic field. In particular, an equilateral triangle with the classical coplanar 120° spin ordering does not have charge redistribution in the ground state due to the C_3 symmetry of the spin structure. However, for an easy-plane anisotropy, an in-plane magnetic field perpendicular to the bond 2–3 cants the spins in such a way that $\langle \mathbf{S}_1 \cdot \mathbf{S}_2 \rangle = \langle \mathbf{S}_1 \cdot \mathbf{S}_3 \rangle$ becomes larger than $\langle \mathbf{S}_2 \cdot \mathbf{S}_3 \rangle$ inducing an electric-dipole moment in the field direction [see Fig. 3(b)]. Thus, a nonzero electric polarization of pure electronic origin appears in such nonsymmetric spin configuration.²³ It is important to note that for an extended lattice, the charge on a given site is a sum of contributions coming from all the triangles that contain such site.

The projected dipole and current operators are identically zero for *bipartite* lattices with nearest-neighbor hoppings.²⁴ This results from the invariance of H under the product of particle hole and hopping $t \rightarrow -t$ transformations, while \mathbf{P} and \mathbf{I} are odd under this transformation. Thus, in perturbation series in t/U , the only terms that contribute to \mathbf{P} and \mathbf{I} originate from loops with odd number of hoppings.

The electric dipole induced by virtual electron hopping has the same form as the one resulting from the dependence of the exchange constants on ion displacements \mathbf{u}_i (magnetostriction): $J_{ij} \approx J_{ij}(0) + \mathbf{u}_n \cdot \nabla_{\mathbf{u}_n} J_{ij}$. Minimizing the sum of the magnetic energy $\sum J_{ij} \mathbf{S}_i \cdot \mathbf{S}_j$ and the lattice distortion energy with respect to \mathbf{u}_i , we find that the resulting electric dipole of a triangle is expressed in terms of scalar products $\mathbf{S}_i \cdot \mathbf{S}_j$. Due to the symmetry considerations discussed above, the spin structure of the dipole is the same as in Eq. (8), while the coefficient is $\sim e|\nabla_{\mathbf{u}_n} J|/K$, where K is the lattice spring constant. The estimate for this coefficient is eaJ/U , i.e., the magnetostriction contribution to the dipolar moment may be larger by a factor of order t/U . Electronic dipoles, $\tilde{\mathbf{P}}_e$, corresponding to Eq. (8), together with the spin-dependent dipoles originating from magnetostriction lead to the coupling between spins and electric field (eZ_l is the charge of an ion l):

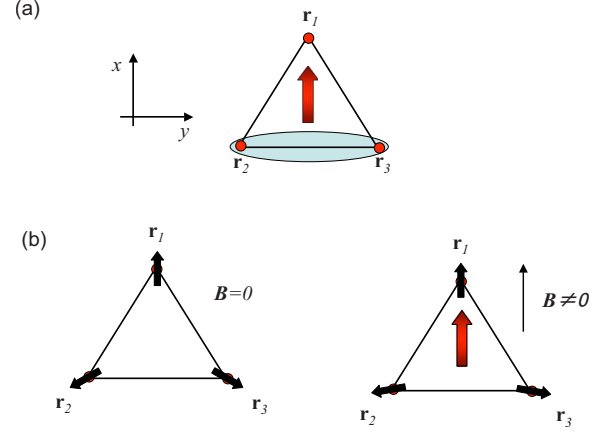


FIG. 3. (Color online) (a) Example of magnetic state with nonzero polarization indicated by the arrow. The two spins inside the oval form a singlet and the unpaired spin can be up or down. This is one of the degenerate ground states of the antiferromagnetic Heisenberg Hamiltonian on an equilateral triangle, which according to Eq. (8), has a nonzero electric-dipole moment. (b) Example of electric polarization induced by a magnetic field \mathbf{B} .

$$\tilde{H}_e = -\tilde{\mathbf{P}} \cdot \mathbf{E}, \quad \tilde{\mathbf{P}} = \tilde{\mathbf{P}}_e + \sum_{ijl} eZ_l K_l^{-1} (\mathbf{S}_i \cdot \mathbf{S}_j - 1/4) \nabla_{\mathbf{u}_l} J_{ij}. \quad (9)$$

III. CHARGES AND CURRENTS IN THE GROUND STATE

There are many physical consequences of our main results Eqs. (6) and (7). We start by discussing the static consequences for the ground state. According to our results, spontaneous currents and corresponding orbital moments should appear for nonzero scalar chirality, e.g., for noncoplanar spin textures. Typical examples were already shown in Fig. 1. For lattice systems, the contributions from adjacent triangles to the current on a given bond may cancel each other even when each triangle has nonzero spin chirality. When this cancellation does not occur, a long-range ordered pattern of chiralities leads to a corresponding ordering of currents according to Eq. (6). As it was mentioned in Sec. I, chiral ordering can exist even in the absence of spin ordering.¹⁸ Two widely discussed structures in kagome lattices are those with homogeneous vector chirality, $\kappa_{123} = \langle \mathbf{S}_1 \times \mathbf{S}_2 + \mathbf{S}_2 \times \mathbf{S}_3 + \mathbf{S}_3 \times \mathbf{S}_1 \rangle$ ($\mathbf{q}=0$ structure), and with staggered vector chirality ($\sqrt{3} \times \sqrt{3}$ structure).^{9,25,26} In both cases, if there is an easy-plane anisotropy, the umbrella structure induced by a magnetic field perpendicular to the lattice has nonzero orbital moments. As shown in Fig. 4, the pattern of currents and orbital moments is uniform in the first case, and staggered for the latter case (despite the fact that the net spin moment is the same). The coupling of the net orbital moment to an external magnetic field favors the uniform state.

According to Eq. (7), certain bond-ordered spin structures will lead to a charge redistribution, or spin-driven charge-density wave (S-CDW), which, in particular, can lead to ferroelectricity. The basic effects are already illustrated in Fig. 3. There are many compounds, known as trinuclear spin

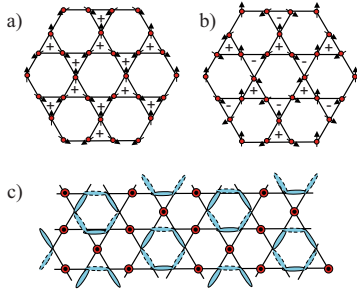


FIG. 4. (Color online) Spin configurations on a kagome lattice that lead to a current or charge ordering in an applied magnetic field. a) The “umbrella” phase induced by a field perpendicular to the plane has a uniform current ordering. The \pm signs denote directions of current. (b) The same as (a) for staggered current ordering. (c) Spin ordering induced by field for a Heisenberg model on a kagome lattice.^{25,26} The elongated ovals indicate a resonating valence bond state on the corresponding hexagons, while the little circles represent spins that are polarized along the field direction. This structure is accompanied by charge ordering: the charges on sites belonging to hexagons and those on isolated sites should be different.

complexes, that contain such isolated triangles. Triangular clusters exist in magnetic molecules such as “V15” $\text{K}_6[\text{V}_{15}^{\text{IV}}\text{As}_6\text{O}_{42}(\text{H}_2\text{O})] \cdot 8\text{H}_2\text{O}$ (Ref. 27) or form well-ordered solids. In particular, the magnetic structure found in $\text{La}_4\text{Cu}_3\text{MoO}_{12}$ (Ref. 28) should, according to Eq. (8), give rise to charge redistribution with nonzero total electric polarization, i.e., this system should be multiferroic. A simple example of a spin-driven charge modulation is given by the 1/3 plateau phase of the $S=1/2$ kagome lattice. This state has the local structure shown in Fig. 4(c), with a resonating singlet state on the hexagons and up spins in between,²⁵ and could be a long-range ordered valence-bond crystal.²⁶ A similar situation arises for the several magnetization plateaus in the Shastry-Sutherland system $\text{SrCu}_2(\text{BO}_3)_2$.²⁹ The states at each plateau consist of ordered arrays of singlet and triplet dimers which according to Eq. (8) should lead to a spin-driven charge density wave.

When magnetic ordering breaks inversion symmetry, the concomitant charge redistribution gives rise to net electric polarization. A simple example is provided by the saw-tooth chain formed by corner-sharing triangles (see Fig. 5).³⁰ Due to the inequivalence of the A and B sublattices, the induced electric charges q_A and q_B are different even in the disordered spin state. For some ratios between the nearest-neighbor A - A and A - B AFM exchange interactions, the spin-1/2 saw-tooth chain has the dimerized ground state.³¹ $\langle \mathbf{S}_n \cdot \mathbf{S}_{n+1} \rangle = \alpha + \beta(-1)^n$, which results in an additional charge redistribution (see also Refs. 32 and 33). The presence of the site and bond density waves breaks inversion symmetry^{33,34} and gives rise to electric polarization along the chain,

$$\tilde{P} = 24ea(t_{AB}^2 t_{AA} / U^3) \beta \quad (10)$$

per triangle, where a is the distance between two neighboring A sites.

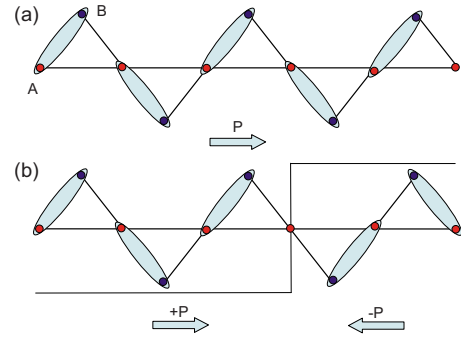


FIG. 5. (Color online) (a) Ferroelectricity induced by dimerization of a sawtooth chain. (b) Domain boundary between two degenerate ground states.

Elementary excitations in dimerized chains are domain walls (kinks) between two degenerate ground states. These topological excitations carry spin 1/2 localized at the domain boundary [see Fig. 5(b)]. Since kinks in the saw-tooth chain are also 180° domain walls separating two ferroelectric domains with opposite polarizations, they carry an electric charge, $Q = \pm 2P/a$, independent of details of the kink’s spin structure (see also Ref. 33). Kinks in isolated chains are mobile^{35,36} and can carry spin *and* charge.

IV. DYNAMICAL PROPERTIES OF MAGNETIC STATES

The dependence of orbital currents and dipole moments on the spin structure leads to an interplay between magnetic and electric dynamical properties of Mott insulators. One can easily show, see Eq. (12) below, that the electric-dipole moment has nondiagonal matrix elements between states with opposite chiralities. Consequently, there will appear dipole-active transitions between states with different chiralities. This immediately leads to a number of interesting consequences.

In first place, the responses of Mott insulators to ac electric and magnetic fields become quantitatively similar. The matrix elements of $\tilde{\mathbf{P}}$ between the ground state, $|0\rangle$, and excited magnetic states, $|n\rangle$, define the contribution of these states to the dielectric function,

$$\epsilon_{ik}(\omega) = \epsilon_0 \delta_{ik} - \frac{8\pi}{V} \sum_n \frac{\omega_{n0} \langle 0 | \tilde{P}_i | n \rangle \langle n | \tilde{P}_k | 0 \rangle}{(\omega^2 - \omega_{n0}^2 - i\delta)}, \quad (11)$$

at $T=0$ and frequencies well below the frequencies of optical phonons. Here $\delta \rightarrow 0$, $\hbar \omega_{n0} = E_n - E_0$, $\tilde{H} |n\rangle = E_n |n\rangle$, ϵ_0 is the contribution of all the other high-frequency modes, and V is the total volume. The expression for the magnetic response function, $\mu_{ik}(\omega)$, is obtained by replacing ϵ_0 with μ_0 and $\tilde{\mathbf{P}}$ with $g\mu_B \mathbf{S}$ (we neglect the effect of $\tilde{\mathbf{L}}$ relative to the spin contribution and the difference between $\tilde{\mathbf{S}}$ and \mathbf{S}). The matrix elements of $\tilde{\mathbf{P}}$ are of order $8eat^3/U^3$ for the electronic contribution (and eat^2/U^2 for magnetostriction), i.e., about the same order of magnitude as the matrix elements of $g\mu_B \mathbf{S}$ for $J \sim 100$ K. Here, a is a characteristic interatomic distance. Hence, the response of a Mott insulator to an ac electric field

may be similar in magnitude to the response to an ac magnetic field.

In second place, the presence of orbital currents in the ground state leads to circular dichroism or rotation of the electric-field polarization. Indeed, if $|0\rangle$ is an eigenstate of \tilde{L}_z with nonzero eigenvalue (orbital currents), there are matrix elements, $\langle 0|\tilde{P}_x|n\rangle$ and $\langle n|\tilde{P}_y|0\rangle$, that are simultaneously nonzero. This is a consequence of the fact that current and polarization are associated with conjugate variables (angular momentum and phase). This rotation of the electric-field polarization is almost the same as Faraday rotation induced by spins on the ac magnetic-field polarization. Hence, it is possible to detect orbital currents (scalar spin chirality) by measuring the rotation of the electric-field polarization.³⁷

In third place, $\epsilon_{ik}(\omega)$ and $\mu_{ik}(\omega)$ may have a common pole. If this situation is accompanied by weak dissipation, both quantities are negative for frequencies slightly below the resonance, leading to a negative refraction index.³⁸ In the isotropic case, the states $|n\rangle$ have well defined total spin S and z -projection S_z . The operator \mathbf{P} preserves these quantum numbers. In contrast, S_x and S_y connect states with different total spin. Therefore, the excited states that contribute to $\epsilon_{ik}(\omega)$ and $\mu_{ik}(\omega)$ are different in general, and the corresponding resonances appear at different frequencies. A nonzero spin-orbit interaction couples the spin and the scalar chirality (orbital currents): it lowers the energy of the states with opposite spin and chiral moments while it increases the energy of states with the same orientation of the spin and chiral moments. Consequently, if the energy spectrum has a Kramers degeneracy, the corresponding eigenstates will have opposite spin *and* scalar spin chiralities. In such case, ac magnetic or electric fields will induce transitions between the same pair of doublets (same frequency) although different pairs of states: an ac magnetic field changes the spin without changing the scalar spin chirality, while an ac electric field changes the scalar chirality without changing the spin. In both cases, the relative spin and chiral orientation is changed leading to common resonance frequencies for $\epsilon_{ik}(\omega)$ and $\mu_{ik}(\omega)$.

The single triangle provides the simplest case for illustrating the aforementioned properties. In absence of Dzyaloshinsky-Moriya (DM) coupling, the ground state of the $S=1/2$ equilateral triangle with antiferromagnetic Heisenberg interactions is a quartet with total spin $S_T=1/2$; the extra degeneracy is due to the scalar chirality [Eq. (1)] that can be positive or negative. The higher energy $S_T=3/2$ quartet is separated from the ground-state quartet by a gap $3J/2$. The full space of the low-energy quartet can be described as a direct product of spin and pseudospin variables. By using the expressions (6) and (8) for the orbital current, \tilde{P}_x and \tilde{P}_y in terms of spin operators, we find that

$$\tilde{P}_x = -CT_x, \quad \tilde{P}_y = CT_y, \quad (\hbar a/U)\tilde{I} = T_z, \quad (12)$$

where $C=12\sqrt{3}ea(t/U)^3$ and (T_x, T_y, T_z) are Pauli matrices that operate in the pseudospin subspace. [We recall that, according to Eq. (6), T_z is proportional to the scalar spin chirality (1).] The resulting SU(2) commutation relations, $[T_\mu, T_\nu] = i\epsilon_{\eta\mu\nu}T_\eta$ for the current and polarization operators is

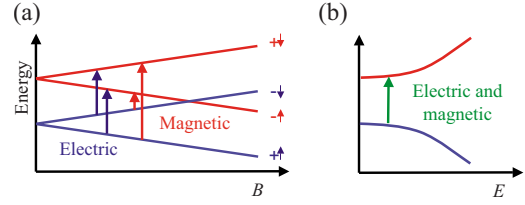


FIG. 6. (Color online) Magnetic energy levels of a single triangle with Dzyaloshinsky-Moriya interaction. (a) As a function of applied dc magnetic field. Blue (red) arrows show transitions induced by ac electric (magnetic, EPR) field. (b) As a function of a dc electric field.

a consequence of the projection and the fact that they are conjugate variables. From Eq. (12) we immediately see that an electric field has nondiagonal matrix elements and will lead to transitions between states with opposite chiralities. Note, that the commutator of \tilde{P}_x and \tilde{P}_y does not vanish in the restricted S subspace, although P_x and P_y commute in the original Hilbert space of H . Note also that the eigenstates of T_z break the time-reversal symmetry [see Fig. 1(a)], while the eigenstates of \tilde{P}_x [see Fig. 3(a)] and \tilde{P}_y , which are linear combinations of states with opposite spin chirality, break the spatial C_3 symmetry. The states in the lowest-energy quartet, $|\chi, \sigma\rangle$, are labeled by their pseudospin (i.e., scalar chirality) and spin projections: $T_z T = \pm 1$ and $S_T^z = \pm 1/2$ ($\sigma = \uparrow$ or \downarrow).

In some real systems such as V15 (see Ref. 27), the lattice symmetry allows for a nonzero DM coupling $H_{DM} = \sum_{ij} \mathbf{D}_{ij} \cdot [\mathbf{S}_i \times \mathbf{S}_j]$. In V15 the $S_T=1/2$ quartet is separated from the $S_T=3/2$ quartet by a gap $\Delta_{3/2} \sim 2.6 \text{ cm}^{-1}$. The terms that mix the $S=1/2$ and $S=3/2$ states (with in-plane components of the vector \mathbf{D}_{ij}) are relatively small. On the other hand, the D_z term plays the role of a spin-orbit coupling between the spin and the orbital moment \tilde{L}_z , and splits the ground-state quartet into two doublets $\{ |+, \uparrow\rangle, |-, \downarrow\rangle \}$ and $\{ |+, \downarrow\rangle, |-, \uparrow\rangle \}$, by an energy $\Delta = \sqrt{3}D_z \sim 0.24 \text{ cm}^{-1}$ (see Fig. 6). Consequently, the system exhibits the following properties:

I. As follows from Eqs. (6), (9), and (12), an ac electric field induces transitions between states with opposite chirality (opposite T_z). In absence of a static magnetic field, this dipole-allowed microwave absorption has the same resonance frequency, $\omega_0 = \Delta/\hbar$, as the usual electron-spin-resonance (ESR) line, and the intensities are comparable. Thus we have here a new dipole-active “ESR”-like transition, caused not by the magnetic field but by the electric component of an ac electromagnetic field. In a static magnetic field, B , the absorption frequency due to the ac electric field remains the same, while the ESR frequency splits linearly in B [see Fig. 6(a)]. On the other hand, an electric field mixes and splits states with the same spin and opposite chirality, increasing the frequency of the usual ESR and of the new electric microwave transitions [see Fig. 6(b)].

II. Slightly below ω_0 , both $\epsilon_{ii}(\omega)$ and $\mu_{ii}(\omega)$ ($i=x, y$) are negative if dissipation is weak, leading to a negative refraction index.

III. The off-diagonal elements $\epsilon_{xy}(\omega)$ and $\epsilon_{yx}(\omega)$ are nonzero at low temperatures in the presence of a magnetic field which splits the lowest-energy doublet. This results in a

strong rotation of the electric-field polarization at frequencies of order ω_0 .

IV. The electric field causes transitions between states with the same total spin. Therefore, $\epsilon_{ik}(\omega)$ changes with the ground-state magnetization until the contribution of magnetic states vanishes when all spins become aligned in the field direction. Hence, measurements of the dielectric response, including the dielectric constant $\epsilon_{ab}(0)$, as a function of magnetic field will provide information about the structure of the magnetic spectrum. According to Eq. (11), for $\tilde{P} = eaJ/U \sim 10^{-4}ea$, we estimate the magnetic states contribution to $\epsilon_{ab}(0)$ as $\langle \tilde{P} \rangle^2 N/\Delta \sim 0.01$ (where N is the concentration of molecules). For V15 this contribution vanishes for fields $H > 3$ T because the $S_T^z = 3/2$ state becomes the ground state.

In conclusion, we showed that the standard viewpoint for the low-energy states of Mott insulators is, in general, incorrect: charge degrees of freedom, which are still active at low energies, can lead to electric orbital currents or charge modulations. These electrical properties of Mott insulators distinguish them from the standard band insulators. The charge ordering can exhibit electric-dipole moments, providing a purely electronic mechanism of multiferroic behavior. In addition, the low-energy magnetic states also contribute to the low-frequency optical properties, such as a dipole-allowed absorption by magnetic excitations well below the Hubbard gap. An even more striking property is the possibility of having persistent electronic orbital currents in the ground state of Mott insulators. The corresponding orbital moments can be detected by measuring the resulting rotation of the electric-field polarization or by nuclear-magnetic resonance.

ACKNOWLEDGMENTS

We thank A. Saxena for useful discussion. LANL is supported by U.S. DOE under Contract No. W-7405-ENG-36. The work of D.Kh. was supported by the DFG via SFB 608 and the European project COMEPHS.

APPENDIX: DEGENERATE PERTURBATION THEORY

Here, we derive the effective current and charge operators [Eqs. (6) and (7)] for the low-energy subspace of the half-filled Hubbard model (Eq. (2)) in the large U/t limit. The low-energy subspace for $t=0$ is generated by all the states $\{|\tilde{\psi}_i\rangle\}$ having exactly one particle on each site (all of them have zero energy). Consequently, any operator acting on this subspace can be expressed in terms of the spin 1/2 operators \mathbf{S}_i . For nonzero t/U , the huge degeneracy is removed to second order in t because the kinetic-energy term mixes the unperturbed states, $\{|\tilde{\psi}_i\rangle\}$, with states containing empty and double-occupied sites. Since the perturbed low-energy states, $\{|\psi_i^n\rangle\}$, (n is the order of the perturbation theory) are adiabatically connected with the unperturbed spin states, $|\tilde{\psi}_i\rangle = e^S |\psi_i\rangle$, the projection of any physical operator O onto the subspace \mathcal{S} generated by the perturbed low-energy states can still be expressed as a function of the spin operators \mathbf{S}_i . The

projected or low-energy effective operator will be denoted as \tilde{O} . The expression for \tilde{O} is:

$$\tilde{O} = \mathcal{P}e^S O e^{-S}\mathcal{P}, \quad (\text{A1})$$

where the anti-Hermitian matrix S is the infinitesimal generator of the canonical transformation, and \mathcal{P} is the projector onto the low-energy subspace \mathcal{S} . In particular, this expression implies that:

$$\langle \psi_i | O | \psi_j \rangle = \langle \tilde{\psi}_i | \tilde{O} | \tilde{\psi}_j \rangle \quad (\text{A2})$$

In particular, when O is the Hamiltonian, we have:

$$\tilde{H} = \mathcal{P}e^S H e^{-S}\mathcal{P}. \quad (\text{A3})$$

The operator S is determined by requiring that \tilde{H} must not contain any term of lower order than t^n , where n is the order up to which the perturbation theory is valid. The Heisenberg Hamiltonian $\tilde{H}^{(2)}$ is obtained by expanding Eq. (A3) up to order t^2 .

In certain cases, it is not necessary to compute the operator S because the expression of \tilde{O} is determined by the symmetry properties of O up to a few constants that can be determined by using Eq. (A2). This is the case of the current and the charge operators as we will see below.

The shortest closed loop for obtaining nonvanishing current and polarization operators is a triangle, i.e., a perturbative expansion involving three hopping processes. Therefore, if we are only interested in the lowest-order nontrivial (non-zero) contribution, it is enough to compute our effective operators for a single triangle and then add the contributions from different triangles that are common to a given site (for the charge operator) or a given bond (for the current operator). The low-energy subspace of a single triangle of sites a, b, c is described by the spin operators $\mathbf{S}_a, \mathbf{S}_b$ and \mathbf{S}_c . Since the charge is a scalar and the current a vector which is odd under time reversal, the only possible expressions involving three spins operators are:

$$\tilde{\mathbf{I}}_{ab,c} = \frac{e\mathbf{r}_{ab}}{\hbar r_{ab}} \gamma \mathbf{S}_c \cdot (\mathbf{S}_a \times \mathbf{S}_b) \quad (\text{A4})$$

$$\tilde{n}_a = 1 + \beta(\mathbf{S}_a \cdot \mathbf{S}_b + \mathbf{S}_a \cdot \mathbf{S}_c) + \beta' \mathbf{S}_b \cdot \mathbf{S}_c. \quad (\text{A5})$$

Here, we have also used the spatial symmetry of the equilateral triangle in the second equation (the coefficients of $\mathbf{S}_a \cdot \mathbf{S}_b$ and $\mathbf{S}_a \cdot \mathbf{S}_c$ must be the same). Since the charge on each site is exactly equal to one for the state that has total spin $S_T = 3/2$, we obtain $\beta' = -2\beta$. Therefore, the current and charge operators are completely determined by the parameters γ and β , respectively:

$$\tilde{\mathbf{I}}_{ab,c} = \frac{e\mathbf{r}_{ab}}{\hbar r_{ab}} \gamma \mathbf{S}_c \cdot (\mathbf{S}_a \times \mathbf{S}_b) \quad (\text{A6})$$

$$\tilde{n}_a = 1 + \beta(\mathbf{S}_a \cdot \mathbf{S}_b + \mathbf{S}_a \cdot \mathbf{S}_c - 2\mathbf{S}_b \cdot \mathbf{S}_c), \quad (\text{A7})$$

A. Determination of β

The perturbative expansion in t/U for the coefficients γ and β can be computed in the following way. We first define an orthonormal set of four wave functions that generate an invariant subspace of the original Hubbard Hamiltonian H generated by the $S_T=1/2$, $S_T^z=1/2$ states which are antisymmetric under exchange of sites b and c :

$$\begin{aligned} |\phi_{1a}\rangle &= \frac{1}{\sqrt{2}}(c_{a\uparrow}^\dagger c_{b\uparrow}^\dagger c_{c\downarrow}^\dagger - c_{a\uparrow}^\dagger c_{b\downarrow}^\dagger c_{c\uparrow}^\dagger)|0\rangle \\ |\phi_{2a}\rangle &= \frac{1}{\sqrt{2}}(c_{a\uparrow}^\dagger c_{b\uparrow}^\dagger c_{b\downarrow}^\dagger - c_{a\uparrow}^\dagger c_{c\uparrow}^\dagger c_{c\downarrow}^\dagger)|0\rangle \\ |\phi_{3a}\rangle &= \frac{1}{\sqrt{2}}(c_{a\uparrow}^\dagger c_{a\downarrow}^\dagger c_{b\uparrow}^\dagger - c_{a\uparrow}^\dagger c_{a\downarrow}^\dagger c_{c\uparrow}^\dagger)|0\rangle \\ |\phi_{4a}\rangle &= \frac{1}{\sqrt{2}}(c_{b\uparrow}^\dagger c_{c\uparrow}^\dagger c_{c\downarrow}^\dagger - c_{b\uparrow}^\dagger c_{b\downarrow}^\dagger c_{c\uparrow}^\dagger)|0\rangle. \end{aligned} \quad (\text{A8})$$

This subspace contains the low-energy spin state $|\tilde{\psi}_{1a}\rangle = |\phi_{1a}\rangle$ which is the only state that has no double-occupied sites in this set of four. It is illustrated in Fig. 3(a) and has a nonzero mean value of $1-\tilde{n}_a$ (i.e., nonvanishing polarization). This state has nonzero matrix elements of H with the high-energy states $|\phi_{2a}\rangle$, $|\phi_{3a}\rangle$, and $|\phi_{4a}\rangle$, that have the same symmetry and contain one double-occupied site. Therefore, for nonzero t/U , the ground state of H , $|\psi_{1a}\rangle$, is a linear combination of the four states:

$$|\psi_{1a}\rangle = \sum_{i=1,4} \alpha_i |\psi_{ia}\rangle. \quad (\text{A9})$$

By using that $\langle \tilde{\psi}_{1a} | \tilde{n}_a | \tilde{\psi}_{1a} \rangle = \langle \psi_{1a} | n_a | \psi_{1a} \rangle$, we obtain $\beta = \frac{2}{3}(1 - \alpha_1^2 - \alpha_2^2 - 2\alpha_3^2)$.

The Hubbard Hamiltonian is represented by the following matrix in the basis of states given in Eq. (A8):

$$\begin{pmatrix} 0 & 2t & -t & -t \\ 2t & U & -t & t \\ -t & -t & U+t & 0 \\ -t & t & 0 & U-t \end{pmatrix}$$

Using this matrix we can compute the coefficients α_i as a power expansion in t/U :

$$\begin{aligned} \alpha_1 &= 1 + \sum_{j=1}^{\infty} a_j \left(\frac{t}{U}\right)^j & \alpha_2 &= \sum_{j=1}^{\infty} b_j \left(\frac{t}{U}\right)^j \\ \alpha_3 &= \sum_{j=1}^{\infty} c_j \left(\frac{t}{U}\right)^j & \alpha_4 &= \sum_{j=1}^{\infty} d_j \left(\frac{t}{U}\right)^j. \end{aligned} \quad (\text{A10})$$

By solving $H|\psi_{1a}\rangle = \epsilon|\psi_{1a}\rangle$ up to second order in t , we obtain the following values of the coefficients a_j , b_j , c_j , and d_j :

$$a_1 = 0, \quad b_1 = -2, \quad c_1 = 1, \quad d_1 = 1,$$

$$a_2 = -3, \quad b_2 = 0, \quad c_2 = -3, \quad d_2 = 3, \quad (\text{A11})$$

with $\epsilon = -6t^2/U + \mathcal{O}(t^4/U^3)$.

In this way, we obtain β to the lowest order in t/U :

$$\beta = \frac{-4t^3}{3U^3}(b_1 b_2 + 2c_1 c_2) + \mathcal{O}\left(\frac{t^5}{U^5}\right) = 8\frac{t^3}{U^3} + \mathcal{O}\left(\frac{t^5}{U^5}\right). \quad (\text{A12})$$

The generalization of this result to the case of three different hopping amplitudes, t_{ab} , t_{bc} , and t_{ca} , is:

$$\beta = 8\frac{t_{ab}t_{bc}t_{ca}}{U^3} + \mathcal{O}\left(\frac{t^5}{U^5}\right). \quad (\text{A13})$$

This results from the fact that the three hoppings t_{ij} must be involved to close the loop.

B. Determination of γ

We proceed in a similar way for computing the coefficient of the current operator. In this case, we consider the following orthonormal set of three $S_T=1/2$, $S_T^z=1/2$ wave functions that are eigenvalues of the C_3 rotation by $2\pi/3$ with eigenvalue $e^{i\alpha}$ ($\alpha=2\pi/3$) and generate an invariant subspace of H :

$$\begin{aligned} |\phi_1\rangle &= \frac{1}{\sqrt{3}}(c_{a\uparrow}^\dagger c_{b\uparrow}^\dagger c_{c\downarrow}^\dagger + e^{i\alpha} c_{a\downarrow}^\dagger c_{b\uparrow}^\dagger c_{c\uparrow}^\dagger + e^{-i\alpha} c_{a\uparrow}^\dagger c_{b\downarrow}^\dagger c_{c\uparrow}^\dagger)|0\rangle \\ |\phi_2\rangle &= \frac{1}{\sqrt{3}}(c_{a\uparrow}^\dagger c_{a\downarrow}^\dagger c_{b\uparrow}^\dagger + e^{i\alpha} c_{b\uparrow}^\dagger c_{b\downarrow}^\dagger c_{c\uparrow}^\dagger + e^{-i\alpha} c_{a\uparrow}^\dagger c_{c\uparrow}^\dagger c_{c\downarrow}^\dagger)|0\rangle \\ |\phi_3\rangle &= \frac{1}{\sqrt{3}}(c_{a\uparrow}^\dagger c_{a\downarrow}^\dagger c_{c\uparrow}^\dagger + e^{i\alpha} c_{a\uparrow}^\dagger c_{b\uparrow}^\dagger c_{b\downarrow}^\dagger + e^{-i\alpha} c_{b\uparrow}^\dagger c_{c\uparrow}^\dagger c_{c\downarrow}^\dagger)|0\rangle, \end{aligned} \quad (\text{A14})$$

Again, $|\tilde{\psi}_1\rangle = |\phi_1\rangle$ is a low-energy state that has a nonzero mean value of $\tilde{\mathbf{I}}_{ab,c}$. The Hamiltonian H only connects $|\phi_1\rangle$ with the high-energy states, $|\phi_2\rangle$ and $|\phi_3\rangle$, that have the same symmetry and one double-occupied site. The ground state of H restricted to this subspace has a net current and can be written as:

$$|\psi_1\rangle = \sum_{i=1,3} \xi_i |\phi_i\rangle. \quad (\text{A15})$$

The current operator $\mathbf{I}_{a,b}$ is given in Eq. (5) and its mean value for the ground state $|\psi_1\rangle$ is:

$$\begin{aligned} \langle \psi_1 | \mathbf{I}_{a,b} | \psi_1 \rangle &= \frac{e\mathbf{r}_{ab}}{\hbar\sqrt{3}r_{ab}} \{ -(\xi_1^* \xi_3 + \xi_1 \xi_3^*) \\ &\quad + i[(\xi_1 + \xi_3)\xi_2^* e^{i\phi} + (\xi_1^* + \xi_3^*)\xi_2 e^{-i\phi}] \}, \end{aligned} \quad (\text{A16})$$

where $\phi=5\pi/6$. The coefficient γ is obtained from the identity [see Eq. (A2)]:

$$\frac{\hbar}{e} \langle \psi_1 | I_{a,b} | \psi_1 \rangle = \langle \phi_1 | \gamma \mathbf{S}_c \cdot (\mathbf{S}_a \times \mathbf{S}_b) | \phi_1 \rangle = \frac{\sqrt{3}\gamma}{4}, \quad (\text{A17})$$

which leads to

$$\gamma = \frac{4t_{ab}}{\sqrt{3}} \{ -(\xi_1^* \xi_3 + \xi_1 \xi_3^*) + i[(\xi_1 + \xi_3) \xi_2^* e^{i\phi} + (\xi_1^* + \xi_3^*) \xi_2 e^{-i\phi}] \}. \quad (\text{A18})$$

In this subspace, the Hamiltonian matrix is:

$$\begin{pmatrix} 0 & \sqrt{3}te^{-i\phi} & i\sqrt{3}t \\ \sqrt{3}te^{i\phi} & U & -\sqrt{3}te^{i\phi} \\ -i\sqrt{3}t & -\sqrt{3}te^{-i\phi} & U \end{pmatrix},$$

with $\phi = 5\pi/6$. Again we expand the coefficients ξ_i in powers of t/U :

$$\xi_1 = 1 + \sum_{j=1}^{\infty} a_j \left(\frac{t}{U}\right)^j \quad \xi_2 = \sum_{j=1}^{\infty} b_j \left(\frac{t}{U}\right)^j \quad \xi_3 = \sum_{j=1}^{\infty} c_j \left(\frac{t}{U}\right)^j \quad (\text{A19})$$

and solve the equation $H|\psi_1\rangle = \epsilon|\psi_1\rangle$ up to second order in t , obtaining:

$$\begin{aligned} a_1 &= 0, & b_1 &= -\sqrt{3}e^{i\phi}, & c_1 &= i\sqrt{3}, \\ a_2 &= -3, & b_2 &= 3ie^{i\phi}, & c_2 &= -3, \end{aligned} \quad (\text{A20})$$

By introducing these coefficients in Eq. (A18), we obtain the following expansion for γ :

$$\gamma = 24 \frac{t^3}{U^2} + \mathcal{O}\left(\frac{t^5}{U^4}\right). \quad (\text{A21})$$

Again, the generalization of this result to the case of three different hopping amplitudes t_{ab} , t_{bc} and t_{ca} is:

$$\gamma = 24 \frac{t_{ab}t_{bc}t_{ca}}{U^2} + \mathcal{O}\left(\frac{t^5}{U^4}\right), \quad (\text{A22})$$

because the three hoppings t_{ij} must be involved to close the loop.

*Also at the Loughborough University, Loughborough, United Kingdom

¹M. Fiebig, J. Phys. D: Appl. Phys. **38**, 123 (2005).

²Y. Tokura, Science **312**, 1481 (2006).

³S.-W. Cheong and M. V. Mostovoy, Nat. Mater. **6**, 13 (2007).

⁴D. I. Khomskii, J. Magn. Magn. Mater. **306**, 1 (2006).

⁵C. D. Batista, Phys. Rev. Lett. **89**, 166403 (2002).

⁶X. G. Wen, F. Wilczek, and A. Zee, Phys. Rev. B **39**, 11413 (1989).

⁷R. B. Laughlin, Science **242**, 525 (1988).

⁸D. Grohol, K. Matan, Jin-Hyung Cho, Seung-Hun Lee, Jeffrey W. Lynn, Daniel G. Nocera, and Young S. Lee, Nat. Mater. **4**, 323 (2005).

⁹W. Schweika, M. Valldor, and P. Lemmens, Phys. Rev. Lett. **98**, 067201 (2007).

¹⁰Y. Taguchi, Y. Ohawa, H. Yoshizawa, N. Nagaosa, and Y. Tokura, Science **291**, 2573 (2001), and references therein.

¹¹H. J. Kawamura, J. Phys.: Condens. Matter **10**, 4707 (1998).

¹²H. Kawamura, Phys. Rev. Lett. **68**, 3785 (1992).

¹³H. Nojiri, E. Ishikawa, and T. Yamase, Prog. Theor. Phys. Suppl. **159**, 292 (2005).

¹⁴T. Momoi, K. Kubo, and K. Niki, Phys. Rev. Lett. **79**, 2081 (1997).

¹⁵B. S. Shastry and B. I. Shraiman, Phys. Rev. Lett. **65**, 1068 (1990); P. E. Sulewski, P. A. Fleury, K. B. Lyons, and S. W. Cheong, *ibid.* **67**, 3864 (1991).

¹⁶N. Mermin and H. Wagner, Phys. Rev. Lett. **17**, 1133 (1966).

¹⁷J. A. Villain, J. Phys. (Paris) **38**, 385 (1977).

¹⁸J.-C. Domenge, P. Sindzingre, C. Lhuillier, and L. Pierre, Phys. Rev. B **72**, 024433 (2005).

¹⁹Bogoliubov came very close to this result long ago, by using a perturbative approach with respect to the small parameter t/U to

describe the correlated metallic state. N. N. Bogolyubov, *Lectures on Quantum Statistics* (Gordon and Breach, New York, 1967), p. 120.

²⁰It is important to note that the spin chirality $\chi_{ij,k}$ generates an effective flux for electrons that move in a conduction band and interact with the localized spin via exchange. In other words, a conduction electron that moves around the triangle ijk acquires a Berry phase $\chi_{ij,k}$. However, this well-known phenomenon that produces an anomalous Hall effect (Ref. 10) requires the existence of a conduction band that is not present in a simple Mott insulator. The current operator of Eq. (6) is associated with the same electrons that provide the localized spins.

²¹O. I. Motrunich, Phys. Rev. B **73**, 155115 (2006).

²²P. Lemmens *et al.*, Phys. Rev. Lett. **87**, 227201 (2001).

²³The possibility to induce electric polarization by noncollinear spins—actually by the vector chirality—due to a relativistic spin-orbit coupling was suggested recently by H. Katsura, N. Nagaosa, and A. V. Balatsky, Phys. Rev. Lett. **95**, 057205 (2005) and by I. A. Sergienko and E. Dagotto, Phys. Rev. B **73**, 094434 (2006). Our mechanism of charge redistribution does not require relativistic spin-orbit interaction and should work in any system with appropriate spin structure.

²⁴L. N. Bulaevskii, Sov. Phys. JETP **24**, 154 (1967).

²⁵M. E. Zhitomirsky and H. Tsunetsugu, Prog. Theor. Phys. Suppl. **160**, 361 (2005).

²⁶D. C. Cabra, M. D. Grynberg, P. C. W. Holdsworth, A. Honacker, P. Pujol, J. Richter, D. Schmalfuss, and J. Schulenburg, Phys. Rev. B **71**, 144420 (2005).

²⁷B. Tsukerblat, A. Tarantul, and A. Müller, J. Chem. Phys. **125**, 054714 (2006).

²⁸Y. Qiu, C. Broholm, S. Ishiwata, M. Azuma, M. Takano, R. Bewley, and W. J. L. Buyers, Phys. Rev. B **71**, 214439 (2005).

- ²⁹S. Miyahara and K. Ueda, *J. Phys.: Condens. Matter* **15**, R327 (2003).
- ³⁰I. S. Hagemann, P. G. Khalifah, A. P. Ramirez, and R. J. Cava, *Phys. Rev. B* **62**, R771 (2000).
- ³¹M. W. Long and R. Fehrenbacher, *J. Phys.: Condens. Matter* **2**, 2787 (1990); M. W. Long and S. Siak, *ibid.* **2**, 10321 (1990).
- ³²P. Littlewood and V. Heine, *Solid State Phys.* **12**, 4431 (1979).
- ³³C. D. Batista and A. A. Aligia, *Phys. Rev. Lett.* **92**, 246405 (2004); A. A. Aligia and C. D. Batista, *Phys. Rev. B* **71**, 125110 (2005).
- ³⁴D. V. Efremov, J. van den Brink, and D. I. Khomskii, *Nat. Mater.* **3**, 853 (2004).
- ³⁵T. Nakamura and K. Kubo, *Phys. Rev. B* **53**, 6393 (1996).
- ³⁶D. Sen, B. S. Shastry, R. E. Walstedt, and R. Cava, *Phys. Rev. B* **53**, 6401 (1996).
- ³⁷C. M. Varma, *Phys. Rev. B* **61**, R3804 (2000).
- ³⁸V. G. Veselago, *Sov. Phys. Usp.* **10**, 509 (1968).